Archives of Biochemistry and Biophysics 768 (2025) 110381

Contents lists available at ScienceDirect

Archives of Biochemistry and Biophysics

journal homepage: www.elsevier.com/locate/yabbi

The R337C mutation in the p53 oligomerization domain affects the regulatory domain and its ability to bind response elements: Evidence based on structural and biophysical studies

Alankrita Singh [a], Lakshay Malhotra [a,b], Abhay Mishra [a], Simran Kundral [a], Pawan Kumar Tiwari [a], Saroj Kumar [a], Hariprasad Gururao [a], Punit Kaur [a], Abdul Samath Ethayathulla [a,*]

[a] Department of Biophysics, All India Institute of Medical Sciences, New Delhi, 110029, India
[b] Department of Biochemistry, Sri Venkateswara College, University of Delhi, New Delhi, 110021, India

ARTICLE INFO

Keywords:
p53 oligomerization domain mutant
Tumor suppressor
Differential scanning calorimetry (DSC)
CD spectroscopy
FTIR spectroscopy

ABSTRACT

The homotetrameric form of p53 is critical for performing essential functions like maintaining genomic stability and preventing uncontrolled cell proliferation. In part, these crucial functions are mediated by the p53 C-terminal region (CTR) containing the tetramerization/oligomerization domain (TD/OD) and regulatory domain (RD), responsible for maintaining the protein's oligomeric state and regulating its function. Mutations in the tetramerization domain reduce the transactivation potential and alter the transactivation specificity of p53. This study investigates the effect of high-frequency tetramerization missense mutation p53R337C on protein stability, oligomeric state, and its ability to bind the DNA response elements. For the first time using CD and FTIR spectroscopy, we have shown that the p53 regulatory domain (residues 363–393) and oligomerization domain (residues 327–355) possess a characteristic alpha helix secondary structure, which is enhanced upon binding to DNA, implicating stabilization of the domain. The mutation R337C in the OD impacts the secondary and tertiary structure of p53 CTR, leading to the loss of secondary structure and the formation of unstable tetramers, as shown by CD and DSC thermal studies. Surprisingly, the secondary structure of mutant p53 CTR partially stabilized upon binding to the DNA sequence. Our data suggests that the unstable p53R337C tetramer exhibits weaker binding to the DNA promoter sequence with decreased transcription activity, consistent with previous cell-based assays. Our study conclude that the loss of salt-bridge interactions between Arg337 and Asp352 in the intra-dimer of p53 leads to the formation of unstable tetramers, and the DNA-binding ability of the regulatory domain.

1. Introduction

The tumor suppressor p53 is one of the most essential cellular proteins that plays a vital role in preventing cancer [1,2]. The transcription factor p53 transactivates genes involved in DNA repair [3–6], cell cycle arrest [7–9], and apoptosis [10–12] under stress conditions such as DNA damage [13,14] and oxidative stress [15], thereby preventing uncontrolled proliferation or tumor formation. It consists of 4 domains: the N-terminal transactivation domain (TAD), the central DNA binding domain (DBD), and the C-terminal region comprising the oligomerization domain (OD), and the regulatory domain (RD) [16]. The role of DBD is to bind specific promoters and regulate the expression of various downstream genes in response to cellular stresses [17,18]. Other domains assist the core DBD in carrying out the transactivation function [19–22]. The oligomerization domain is essential for forming a stable tetramer, crucial for p53 activity [23,24], while the regulatory domain is responsible for non-specific DNA binding and scanning for the specific response element [22,25,26].

However, p53 mutations contribute to >50 % of cancer cases, making it the top-most mutated gene causing cancer [27,28]. Interestingly, 72.87 % of these mutations belong to the missense mutations [29]. Approximately 20 % of germline mutations in OD were reported for Li-Fraumeni syndrome (LFS) and ~2 % as somatic p53 mutations [30–33]. Many OD mutations disrupt the ability of p53 to form a

* Corresponding author.
E-mail address: ethayathulla@aiims.edu (A.S. Ethayathulla).

https://doi.org/10.1016/j.abb.2025.110381
Received 1 October 2024; Received in revised form 7 February 2025; Accepted 7 March 2025
Available online 8 March 2025

functional tetramer, and most of them are associated with cancer [34]. Missense mutation in OD accounts for approximately 6 % of p53 related cancers, making OD the second most mutated domain of p53 after DBD (82 %) [29]. Without a functional OD, p53 cannot execute its transcription activity by forming a functional tetramer [35–37]. The degree of loss in transcription activity depends on the location and type of amino acid substitution.

The structure of the p53 OD consists of a β-strand (residue 327–333) and an α-helix (residue 335–355) connected by a single glycine residue at the 334th position. The β-strand of the two monomers interact to form a dimer, stabilized by a crucial salt bridge interaction between Arg337 and Asp352 between monomers. The α-helices of the two dimers form hydrophobic interactions to form a tetramer [38–41]. One of the most frequent mutations affecting the tetramer stability, thereby leading to cancer, is substitution of Arg with Cys at the 337th position [41]. This p53R337C mutation disrupts the salt bridge interaction between Arg337 and Asp352, destabilizing the tetramer. Among all the OD mutants, the p53R337C is reported in various cancers such as esophagus, breast, and kidney cancer ("The TP53 Database | ISB-CGC," n.d.). It is thus essential to characterize the mutant to develop an effective therapy.

So far, there are no substantial studies on the oligomeric state of the mutant p53R337C, and the impact of the mutation on promoter binding is yet to be understood. Some study suggests that the mutant exists as a monomer [31,41,43–47] while others report different oligomeric states such as a dimers, trimers, and tetramers [34,48,49]. Similarly, studies have shown the mutant as partially functional at high concentrations [41,43,47,49–51], whereas others have demonstrated negligible [52–55] to complete loss of transactivation [45,46]. The reported studies have shown that the mutant p53R337C is less thermally stable [34,48], and its transcriptional function is temperature-dependent [51,54]. These studies lack the understanding of how this mutation affects the function of p53. Therefore, we aim to determine the impact of R337C mutation on the secondary and tertiary structure of the oligomerization (OD) and regulatory domain (RD) of p53 in the presence and absence of a DNA promoter to understand whether the mutation affects the DNA binding ability of RD. Using biophysical techniques such as CD spectroscopy, FTIR spectroscopy, and Differential Scanning Calorimetry, we tried to establish the effect of mutation on the p53-CTR.

2. Material and methods

2.1. Cloning, expression, and purification

The wild-type p53 oligomerization and regulatory domain (wtp53 CTR) (residue 318–393) was PCR amplified using full-length wild-type p53 (synthesized by Biogene after codon optimization). The amplified gene was cloned in the pET28a(+) expression vector (Promega, USA) with a C-terminal His tag. The p53R337C CTR mutant was generated by site-directed mutagenesis using wtp53 CTR plasmid as a template, and the sequencing confirmed the mutation. Both recombinant plasmids were transformed in the *E.coli* BL21(DE-3) strain, and the cells were induced with 1 mM IPTG at OD_{600} 0.4–0.6 in 1 L LB at 20 °C for 14 h. The cells were harvested by centrifugation at 5000 rpm for 20 min and stored at −20 °C until use. The cell pellet was resuspended in lysis buffer (20 mM Tris pH-8.0, 500 mM NaCl, 1 mM PMSF, 10 % glycerol), lysed by sonication (amplitude 30, 20 s on and 20 s off cycle for 30 min) using QSonica sonicator, and centrifuged at 13,000 rpm. A pre-equilibrated 1 ml Ni^{2+}-NTA resin was added to the lysate and incubated for batch binding at 4 °C for 1 h. The protein-bound beads were washed twice with lysis buffer and lower concentrations of imidazole buffer. The protein was eluted with 20 mM Tris, pH-8.0, 75 mM NaCl, and 300–500 mM imidazole and further purified using the size exclusion column (Superdex 16/600 75 pg 120 mL) equilibrated with buffer 20 mM Tris, pH-8.0, 75 mM NaCl at 0.5 mL/min flow rate at 4 °C. The purity of the sample was analyzed by 15 % SDS-PAGE and Western Blot using a primary anti-His-Tag Rabbit mAb (Cat no.AE086) and secondary anti-rabbit IgG HRP conjugated goat antibody (Cat no. AS014).

2.2. Effect of pH on CTR secondary structure and CTR secondary structure determination by CD spectroscopy

The CD spectra of wt and mutant-CTR were measured to determine the secondary structure content at different pH conditions using a JASCO J-1500 Spectrophotometer [56–59]. We measured the CD spectra of wtp53-CTR (0.12 mg/mL) and p53R337C-CTR (0.12 mg/mL) in different pH buffers: 10 mM sodium citrate buffer (pH 2–6), 10 mM Phosphate Buffer (pH 7), 10 mM Tris Buffer (pH 8–9), 10 mM Glycine buffer (pH 10–11). We monitored the spectra in the far UV region of 210–250 nm with a 0.2 cm pathlength quartz cuvette with a scan rate of 100 nm/min at 20 °C. For each sample, we measured an average of two spectral scans and the mean residue ellipticity of the spectra was calculated using the following formula:

$$[\theta]_{MRE} = \theta.\ \mathrm{MRW}/c.\mathrm{d}.10$$

Where $[\theta]_{MRE}$ = mean residue ellipticity, θ = measured ellipticity in millidegrees, MRW = mean residue weight of the protein in Da, c = concentration in g/L, d = path length in cm. The MRE spectra were then plotted using SigmaPlot 14.0 and the online server BeStSel [60–63] was used to estimate the secondary structures (for protein spectra at pH-8). The scatter plots of mean residue ellipticity ($degcm^2dmol^{-1}$) at 222 nm and 218 nm representing alpha helix and beta sheet peaks, respectively were generated using SigmaPlot 14.0 for both wt and mutant proteins [58,59].

2.3. Tertiary structure analysis of p53-CTR

The tertiary structure of wtp53 CTR and p53R337C CTR was studied using a fluorescent molecule 8-anilino-1-napthalenesulfonic acid (ANS) in different pH buffers: 10 mM glycine-HCl (pH 2–3), 10 mM acetate (pH 4–5), 10 mM phosphate (pH 6–7), 10 mM tris (pH 8–9), 10 mM glycine-NaOH (pH 10–11). A 10 μM protein was incubated with 200 μM of ANS in the dark at room temperature for 5 min. Fluorescence emission spectra were monitored in triplicate between 400 and 650 nm by exciting the samples at 370 nm using Spectramaxi3x [56]. The fluorescence intensity was plotted against the pH and a scatter diagram was generated with the error bars (n = 3) for pH vs λ max 480 nm using SigmaPlot 14.0.

2.4. Secondary structure analysis of p53 CTR with and without DNA by FTIR spectroscopy

The FTIR spectra of wtp53 CTR (5 mg/mL) and p53R337C CTR (4 mg/mL) were measured in the presence and absence of DNA using a Cary 600 series FTIR spectrometer, Agilent Technologies. The spectra were collected in the wavenumber range of 4000 to 900 cm^{-1} with a resolution of 4 cm^{-1} at room temperature. The FTIR spectra of the p53-CTR in the presence of 26-mer DNA (5′-CGGGCATGCCCTA-TAGGGCATGCCCG-3′) in double-stranded form were recorded in the ratio of 1:1 (500 μM wtp53 CTR and 500 μM of DNA; 800 μM of p53R337C CTR and 800 μM of DNA) in buffer containing 20 mM Tris, pH-8.0 and 75 mM NaCl. We averaged each spectrum for 64 scans, and the secondary structure of the protein was determined by the curve fitting of the second derivative spectra in the amide I region (1700-1600 cm^{-1}). The second derivative and Gaussian curve fitting were performed using the same methodology reported in our previous publication [59].

2.5. Thermal stability of p53-CTR

The thermal stability of both wild-type and mutant p53-CTR proteins was evaluated by circular dichroism (CD) and differential scanning calorimetry (DSC) [64,65]. The thermal denaturation study of wtp53

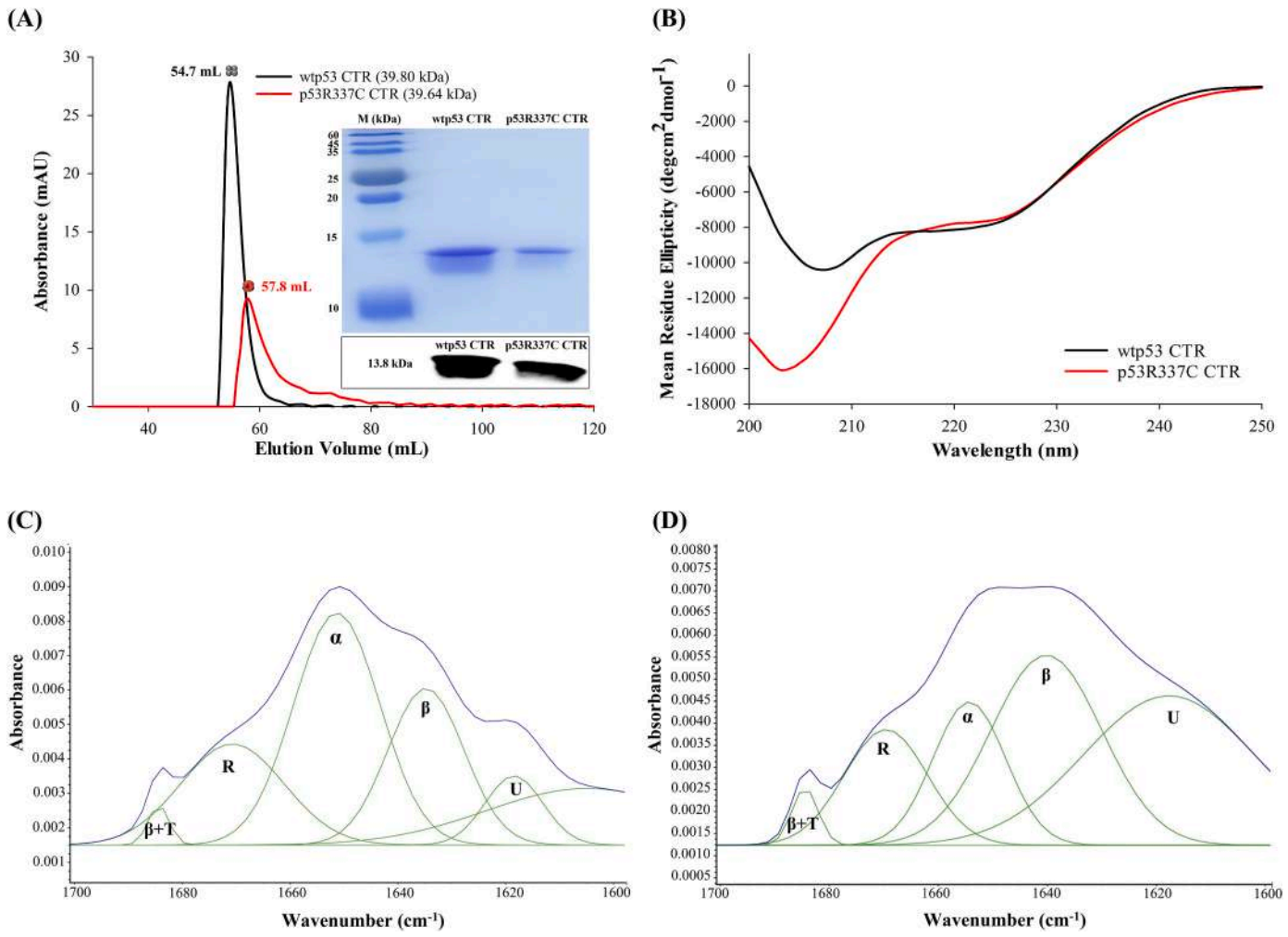

Fig. 1. (A) Size exclusion chromatogram of wtp53 and p53R337C CTR using Superdex 16/600 75 pg column, 15 % SDS PAGE, and Western Blot of purified protein. **(B)** Far UV CD spectra of wtp53 CTR (0.12 mg/mL) and p53R337C CTR (0.12 mg/mL) show differences in mean residue ellipticity. FTIR spectra showing the peak deconvoluted amide I region (1600-1700 cm^{-1}) of **(C)** wtp53 CTR (5 mg/mL) and **(D)** p53R337C CTR (4 mg/mL). The fitted curve (blue) and the deconvoluted peaks (green). (For interpretation of the references to colour in this figure legend, the reader is referred to the Web version of this article.)

CTR (0.12 mg/mL) and p53R337C CTR (0.12 mg/mL) mutant was performed using JASCO J-1500 Spectrophotometer by measuring the ellipticity of proteins at 222 nm over the temperature range of 20–95 °C with the scan rate of 2 °C/min in 0.1 cm pathlength quartz cuvette. The renaturation or reversibility of the protein was determined by rescanning the same sample from 95 to 20 °C. The measured ellipticity was plotted as the function of temperature and the melting temperature (T_m) was calculated using SigmaPlot 14.0.

The thermal stability of wtp53 CTR (1 mg/mL) and p53 R337C CTR (1 mg/mL) was also measured by differential scanning calorimetry using Nano DSC, TA instruments. The change in heat capacity of the proteins was monitored over the temperature range of 20–95 °C with the scan rate of 1 °C/min using Tris buffer (20 mM Tris, pH-8.0, and 75 mM NaCl) as a reference. The molar heat capacity of the protein was calculated using TA NanoAnalyze software, and the baseline correction of the thermogram and the multi-peak Gaussian curve fitting was performed using OriginPro.

2.6. Molecular modeling and Molecular Dynamics(MD) simulation studies

As the crystal structure of p53-R337C OD is not available, the wild-type p53 OD structure (PDB ID: 1AIE, 1.50 Å resolution) was used as a template. Solvent molecules were removed, and Arg337 was substituted with Cys using PyMOL. The p53OD tetramers of both wild-type and mutant were generated and energy minimized using GROMACS- 2023.2. The MD simulations of wtp53 OD tetramer (PDB ID: 1AIE) and p53R337C OD mutant model were performed for 1 μs (3 runs) using GROMACS- 2023.2 using the protocol as described in the previous study [59,66]. The RMSD and RMSF of the MD simulation were calculated and plotted using SigmaPlot 14.0. The free energy landscape (FEL) was computed using the gmx_covar gromacs utility and gmx_anaeig gromacs utility for the generation of the C-alpha covariance matrix and eigenvector, respectively, to generate the FEL plot [66–69].

3. Results

3.1. The mutant p53R337C CTR can form more compact tetramers than wtp53 CTR

A tetramer is the prerequisite form of functional p53; mutation makes the protein defective. By gel filtration chromatography, we observed different tetrameric states of wtp53 and mutant p53R337C CTR with elution volumes of 54.7 mL and 57.8 mL, respectively. A 3 mL difference suggests that the tetrameric state of mutant p53-CTR is more compact and unstable than the wild-type (Fig. 1A and S2A). A stable CTR is required for p53 to bind DNA non-specifically, followed by core domain binding to the specific promoter sequence before the

Table 1
Secondary structure content prediction of wtp53 CTR and p53R337C CTR based on CD spectrum data using online server BeStSel.

Technique	Protein	α- helix (%)	β-sheet (%)		Turns (%)	Random Coil (%)
			Antiparallel	Parallel		
Crystal (8UQR)	wtp53 OD (324–356)	27.5	7.5		2.5	3.75
CD Spectroscopy (BeStSel)	wtp53 CTR (318–393)	31.0	9.3	3.6	13.2	42.9
	p53R337C CTR (318–393)	23.1	15.6	0.0	14.3	47.0

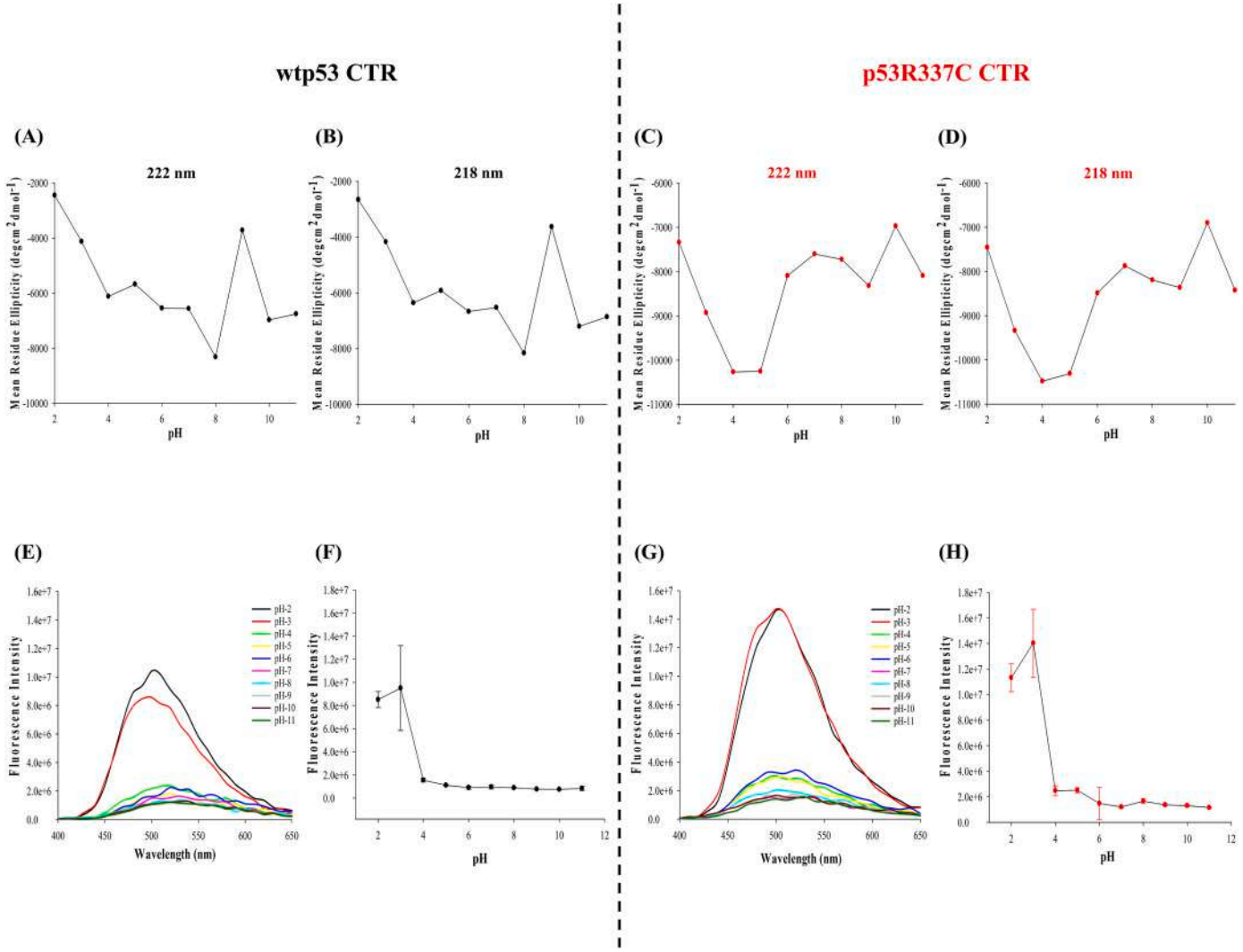

Fig. 2. Scatter plot of wtp53 CTR **(A, B)** and p53R337C CTR **(C, D)** showing Mean Residue Ellipticity (MRE) at 222 nm and 218 nm at different pH conditions. Fluorescence emission spectra of ANS (λ_{ex} 430 nm) binding at different pH along with scatter plots, **(F)** and **(H)** show scatter plots of fluorescence intensity changes at 480 nm upon ANS binding to wtp53 CTR and p53R337C CTR, respectively (n = 3). **(E)** and **(G)** show data from a single replicate of wtp53 CTR and p53R337C CTR, respectively. The spectra indicate that the wt CTR and mutant protein hydrophobic core are intact except at pH 2 and 3.

transcription initiation process is activated [52,70–74]. The loss of the salt bridge between R337 and D352 (Fig. S1) destabilizes the tetramer, reduces the ability and affinity to bind DNA.

3.2. The R337C mutation promotes loss of the secondary structure in p53-CTR

All the structural studies of p53-CTR reported so far lack secondary structure information on the regulatory domain region (residues 363–393) [34,38,73,75,76]. In this study, we measured the CD spectra of p53-CTR (OD + RD) (residues 318–393) in the far UV region and observed a prominent negative peak at 208 nm (π →π* transition) and 222 nm (n→π* transition) characteristic of α-helices (Fig. 1B). Previous reported structural and biophysical studies showed p53 tetramerization domain (residues 324–356) contains 27 % α-helix and 7 % β-sheet [38, 75,77–81]. Our CD spectra of wtp53 CTR shows 31 % α-helix, 12.9 % β-sheet (9.3 % antiparallel and 3.6 % parallel), 13.2 % turns and 42.9 % random coil estimated using the BeStSel server [62]. A 4 % increase in α-helix, ~6 % increase in β-sheet, and 10.7 % turns correspond to the regulatory domain region (residues 363–393) (Table 1). We report the secondary structure content for the entire CTR region (OD + RD) for the first time. However, in the p53R337C mutant, the prominent peak at 208 nm is absent, and a weak negative band at 222 nm suggests an unstable alpha-helical region. Additionally, a distinct negative peak at

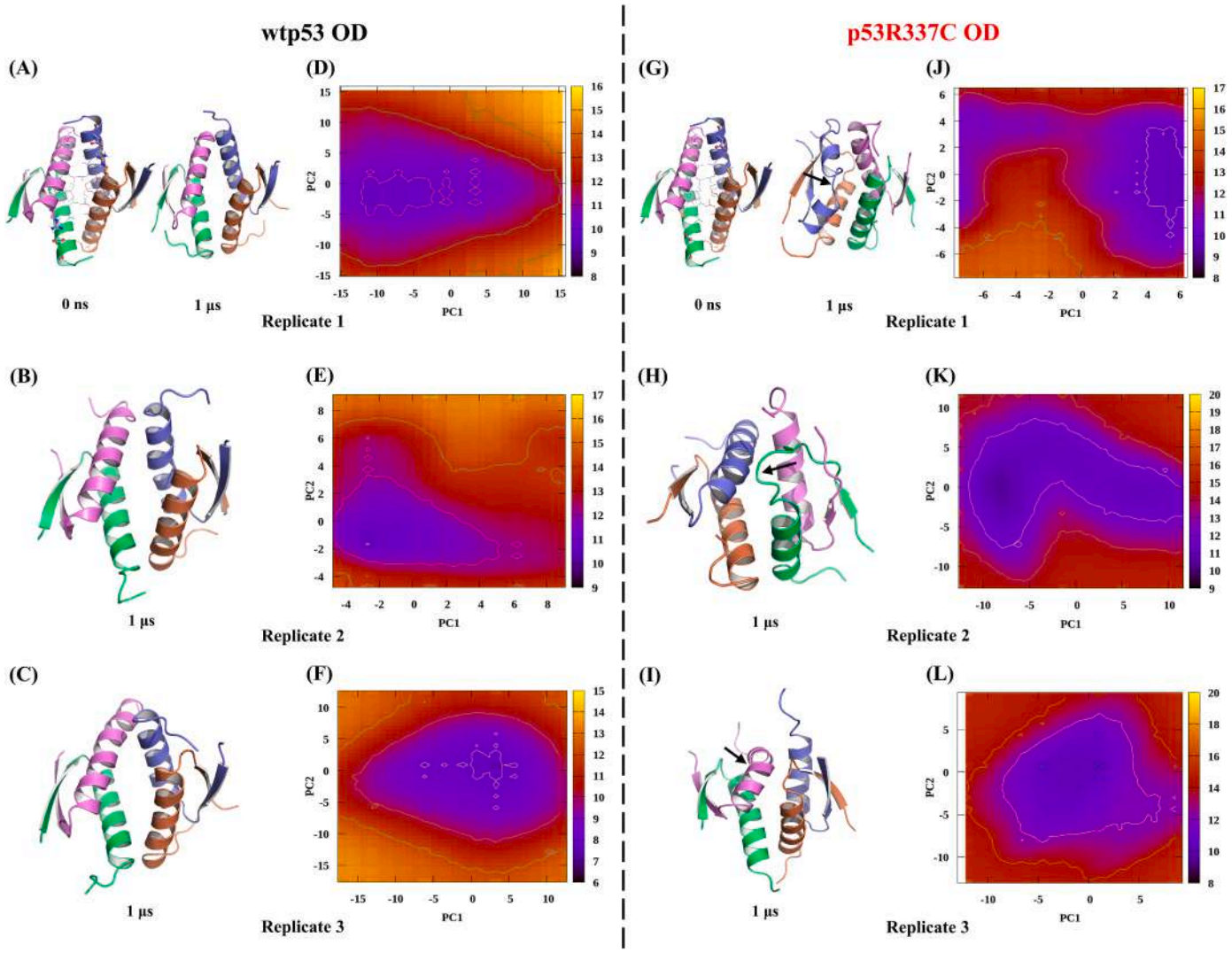

Fig. 3. The MD simulations of wtp53 OD and mutant p53R337C OD. **(A–C)** Represent the 1 µs frame of wtp53 OD, **(G–I)** represents the 1 µs frame of p53R337C OD. The Free Energy Landscape is shown for each MD run of **(D–F)** wtp53 OD and **(J–L)** p53R337C OD.

205 nm in the mutant indicates the presence of a disordered region (Fig. 1B). The secondary structure estimation shows a decrease in alpha-helical content to 23.1 %, an increase in anti-parallel β-sheet (15.6 %), turns (14.3 %) and random coil (47 %). A definite shift of the alpha-helical peak at 208 nm to the random coil at 205 nm implies that the loss of salt bridge interactions between adjacent monomers destabilizes the helix. The destabilized helices significantly impact the regulatory domain's conformation and make the protein unstable; hence, the mutant elutes at different elution volumes in the gel-filtration profile (Fig. 1A).

The change in secondary structure is also observed in the FTIR spectra measured in the mid-infrared region of 4000-900 cm^{-1}. In wtp53 CTR, a characteristic peak of α-helix at 1652 cm^{-1}, β-sheet at 1635 cm^{-1}, β-turn at 1684 cm^{-1}, and random coil at 1673 cm^{-1} along with a peak for the disordered region at 1618 cm^{-1} is observed (Fig. 1C and S4A). In mutant p53R337C CTR, a considerable decrease in secondary structure compared with the wild-type, with the α-helix and β-sheet/strand peaks is observed at 1649 cm^{-1} and 1641 cm^{-1}, respectively. In mutant p53 CTR, a notable band for random coil at 1672 cm^{-1} and a large disordered peak at 1618 cm^{-1} was observed (Fig. 1D and S4B). CD and FTIR data indicate a loss in the α-helical region and an increase in the unstructured region in the mutant leads to an unstable tetramer.

3.3. The p53R337C CTR is more susceptible to pH change

The change in the secondary structure at different pH monitored using the CD spectra shows that the wtp53 CTR is more stable in the pH range from 4 to 8, less stable at pH 9.0 close to isoelectric point (pI-9.69), and unstable below pH 4 (Fig. 2A and B). Meanwhile, the mutant is less stable at pH 8 and lacks wt-like conformation (Fig. 2C and D). Interestingly, the secondary structure signal of the mutant increases at pH 4 and 5, indicating that the protonated cysteine below pH 5.5 might form an H-bond with Asp352 (F ig. 2C and D, S2D and S2E). Similarly, we observe that the spectra of wtp53 CTR below pH 5.0 resemble mutant p53R337C-CTR, indicating that salt-bridge loss destabilizes the protein (Figs. S2B and S2C).

Consequently, we performed ANS binding to check the exposure of the hydrophobic core of p53-CTR tetramers at different pH levels. An increase in fluorescence of ANS at pH-2 and pH-3 indicates that the tertiary structure of both wt and R337C mutant CTR destabilized and exposed the protein's hydrophobic core (Fig. 2E–H). Interestingly, both wtp53 and mutant CTR spectra show that the hydrophobic core is intact and not entirely exposed to ANS binding in the pH range of 4–11. However, at pH 4 and 5, the mutant protein exhibits a minor loss in the tertiary structure, indicating that the mutant tetramer is less stable (Fig. 2G and H). Additionally, p53R337C CTR exhibited higher

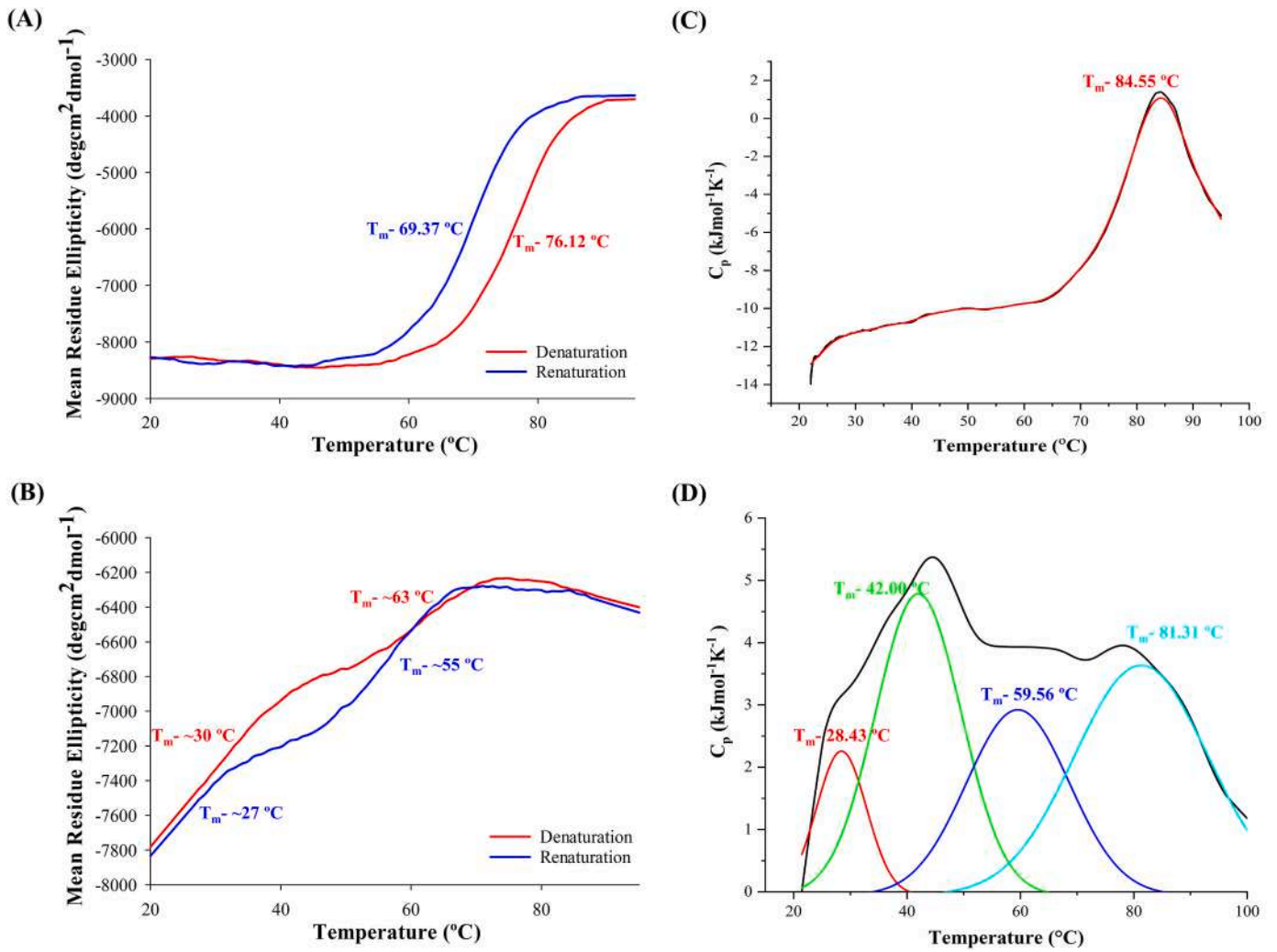

Fig. 4. Thermal stability of wt and mutant p53-CTR region. CD thermal denaturation and renaturation curves of **(A)** wt p53 CTR (0.12 mg/mL) and **(B)** mutant p53R337C CTR (0.12 mg/mL) at 222 nm. DSC thermogram of **(C)** wtp53 CTR (1 mg/mL) and **(D)** p53R337C CTR (1 mg/mL) over the temperature range of 20–95 °C. The DSC thermogram shows the non-fitted (black) and fitted (red) data curve of the wtp53 CTR. The red, green, blue and cyan show the fitted curve of the p53R337C CTR. (For interpretation of the references to colour in this figure legend, the reader is referred to the Web version of this article.)

fluorescence intensity than wtp53 CTR across all pH levels, signifying greater exposure of hydrophobic core (Fig. 2F and H). Hence, the study shows that the mutant forms an unstable tetramer with an intact but more exposed hydrophobic core.

3.4. MD simulations confirm the destabilization of mutant p53 OD tetramers

To study the stability of the p53 OD of both wild-type and mutant, we performed MD simulation of wtp53 and p53R337C OD for 1 μs in triplicate to analyze the impact of the mutation on the structure of the OD. The MD trajectories show that the wtp53 OD remains intact (Fig. 3A–C) throughout 1 μs simulation in all three runs. Structural analysis of salt-bridges formed by R337 in all three replicates of 1 μs MD run revealed that Arginine at position 337 engages in three different interactions: with D352 (~40 %) (intradimer), E349 (~10 %) (intradimer) and E343 (~10 %) (interdimer). It emphasizes that Arginine at 337th position is essential to hold the p53 tetrameric domain (Table S1). In contrast, the α-helix in one of the monomers of p53R337C OD unwinds, thus indicating destabilization of the helix under the influence of this mutation (Fig. 3G–I). The RMSF plots of wild-type shows that the alpha-helical region (335–352) is stable and intact (Figs. S3D–F), whereas in the R337C mutant, destabilization is observed (Figs. S3G–I). Additionally, the RMSD of C_α backbone atoms of the p53R337C is higher than that of wtp53 (Figs. S3A–C). A single local minimum in the free energy landscape plot of wtp53 OD indicates a stable tetrameric conformations (Fig. 3D–F).

In contrast, the mutant shows multiple local minima indicating different conformations due to reduced stabilty (Fig. 3J–L). Therefore, the mutation destabilizes and uncoils the of p53 OD α-helix, which forces the mutant protein to form unstable conformations. The MD data also show that the mutant forms an unstable tetramer with an intact hydrophobic core, as observed in the ANS binding study.

3.5. Mutant p53R337C CTR tetramer is thermally unstable compared with wtp53 CTR

To analyze the thermal stability of wtp53 CTR and mutant-CTR tetramers, we measured the CD spectra at 222 nm in the 20–95 °C temperature range. The wtp53 CTR shows a decrease in the negative ellipticity with the increase in temperature having a T_m of 76.12 °C, followed by complete reversibility of secondary structure upon renaturation (Fig. 4A). For the first time, we have reported the thermal reversibility of wtp53 CTR (OD + RD), indicating that the hydrophobic core of tetramer can refold. In contrast, the mutant shows two different unfolding peaks with T_m of 30 °C and 63 °C, indicating that the unstable

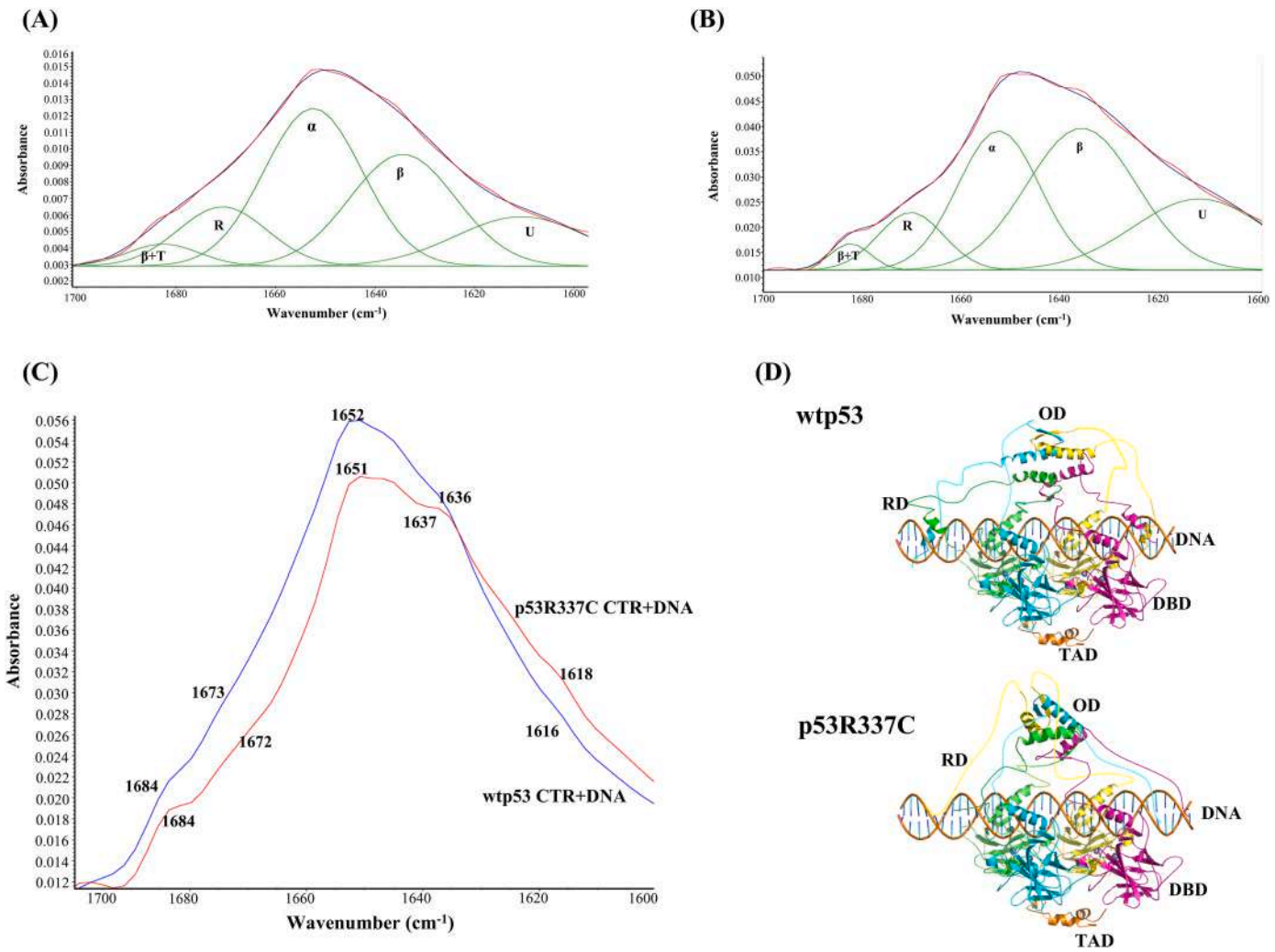

Fig. 5. FTIR spectra of wt and R337C p53-CTR region. The peak deconvoluted amide I region (1600-1700 cm^{-1}) of **(A)** wtp53 CTR (500 μM) in the presence of 26 mer p53 consensus sequence DNA (500 μM) and **(B)** p53R337C CTR (800 μM) in the presence of 26 mer p53 consensus sequence DNA (800 μM). The red line represents the original data, the blue line represents the fitted curve and the green lines represent the deconvoluted peaks. **(C)** The overlay of FTIR spectra of wtp53 CTR and p53R337C CTR in the presence of DNA. **(D)** Diagrammatic representation of the quaternary state model of full-length wtp53 and p53R337C upon binding to the DNA response element. (For interpretation of the references to colour in this figure legend, the reader is referred to the Web version of this article.)

mutant tetramer dissociates into dimers or monomers (Fig. 4B). Furthermore, the mutant exhibits only partial renaturation to its original conformation.

The thermal studies of the wtp53-CTR region by gold-standard differential scanning calorimetry (DSC) also show a single peak at 84.55 ± 0.02 °C (Fig. 4C) with no saturation up to 95 °C, indicating that the protein is highly stable. On the other hand, the mutant shows four different melting peaks at 28.43 ± 0.05 °C, 42 ± 0.12 °C, 59.56 ± 0.25 °C and 81.31 ± 0.28 °C with thermogram approaching to saturation at 95 °C, suggesting complete denaturation of an unstable tetramer of mutant p53R337C CTR (Fig. 4D). Multiple peaks indicate stepwise dissociation of the tetramer into dimer at 42 ± 0.12 °C, and monomer at 59.56 ± 0.25 °C, with final monomer denaturation at 81.31 ± 0.28 °C. Thus, the DSC data further substantiates that the loss of the salt bridge in the mutant leads to a thermally unstable tetramer.

3.6. FTIR spectra of p53-CTR in the presence of DNA

The FTIR spectra of native wtp53 CTR and mutant CTR shows that the wild-type has a characteristic peak of α-helix at 1652 cm^{-1} and β-sheet at 1636, while the mutant exhibits less prominent peaks for α-helix and β-sheet/strand at 1651 cm^{-1} and 1636 cm^{-1}, respectively (Fig. 1C–D). In the presence of DNA, the wtp53 CTR spectra shows an increase in the alpha-helical content with a peak at 1652 cm^{-1} and a decrease in the unstructured region peak at 1616 cm^{-1}, indicating that wild-type binds to the DNA with stable tetramer (Fig. 5A and C, S4A). Surprisingly, the mutant shows a slight increase in the alpha-helical and β-sheet peaks at 1652 cm^{-1} and 1637 cm^{-1}, respectively, along with a decrease in the unstructured region at 1618 cm^{-1} (Fig. 5B and C, S4B). The increase in the secondary structure content of both wtp53 CTR and p53R337C CTR shows that the regulatory region (363–393) stabilizes upon DNA binding.

4. Discussion

During cell stress and DNA damage, over 90 % of p53 forms tetramers [24,82,83]. These tetrameric p53 are activated by post-translational modifications (PTMs), particularly in the C-terminal region [84,85]. These PTMs serve as signals for cellular localization and modulate interdomain and intermolecular interactions of p53 with other pathway proteins [86–89]. Many studies have shown that PTMs in oligomerization and regulatory domain residues act as molecular switches in transforming p53-dependent cellular pathways like apoptosis or cell cycle arrest, thereby regulating cellular outcomes

[89–91]. The oligomeric state is essential for the p53 transactivation function, and mutation inactivates oligomer formation, leading to the non-functional protein [92]. Clinical reports have shown that the oligomeric status impacts clinical outcomes in Li-Fraumeni Syndrome (LFS) patients [31], as the mutations in the oligomeric domain impair the ability to form a tetrameric state or stable tetramers [93]. The crystal structure of OD from the region 324–356 provides insight into the impact of the mutations on the structure of this domain [38,72,78,78,80,94]. Yet, its influence on the regulatory domain (residues 360–393) is poorly understood, as this region is not well characterized due to its intrinsic disorderedness [95,96]. However, the RD domain is essential for the p53 function, as many PTMs are reported in this intrinsically disordered region (IDR) [86,89,97–99]. A recent study by Di Ianni et al. [70] predicted a structural model using mass spectrometry-guided computational modeling, stating that the RD forms a stable structure upon binding to a DNA sequence [70]. Using CD and FTIR, we show that part of the regulatory domain possesses an alpha-helical structure in wtp53 CTR, and it stabilizes upon binding to DNA, as demonstrated by Di Ianni et al. [70]. A small region of stable secondary structure in the RD is required for the post-translation modifications like acetylation, methylation, and phosphorylation to stabilize and form active tetrameric conformation [84,100,101]. We did not observe this stable region in mutant R337C, which might have influenced the functional role of p53.

In vitro studies have found that the mutant R337C was inactive at lower concentrations and partially active at higher concentrations in the reporter gene assay with no activation of downstream target genes [51]. Our thermal studies show that the R337C mutant tetramers are unstable and can dissociate easily into dimer at 42 °C and into monomer at 59.56 °C. At low temperatures, the mutant p53R337C forms tetramer, whereas at around 28.43 °C, the tetramer begins to dissociate; therefore, most of the mutant tetramer dissociates at the physiological temperature of 37 °C. However, at 37 °C, the tetramer is not entirely dissociated, which explains the low transcriptional activity. Hence, a fraction of mutant protein exists in the tetrameric form, enabling it to transactivate the downstream genes. Therefore, mutants mostly form dimers or unstable tetramers with low transcription activity at physiological temperatures. The dimeric or unstable tetrameric mutants exhibit ~80 % cancer penetrance with median survival [35,102]. The study demonstrates that the p53R337C forms an unstable tetramer that can bind the DNA and is partially functional. Therefore, it can be concluded that both wild-type and mutant protein suggest the substitution of Arg to Cys at the 337th position does not prevent the interaction of RD with DNA. However, our experimental data could not establish that the ion pairing between R337 and D352 is critical for the structural stability of p53. Hence, to understand the role of ion pair R337-D352, we analyzed the IARC p53 database (https://tp53.cancer.gov/) [42] for the functional status of p53D352 mutants and found D352 mutants to be functional. Similarly, the study conducted by Kato et al. [40] using yeast-based functional assay also showed that p53D352 mutants (His/Tyr/-Ala/Gly/Val/Glu/Asn) are in active form. Their study showed that the mutation of Arg337 to His was partially functional, while R337L and R337P were non-functional. Hence, the positive charge and length of the side chain of Arg at the 337th position are essential for the structural integrity of p53 to form a full-functional tetramer. We did not observe any Arg to Lys mutation reported in the database to confirm our prediction. However, our 1 μs MD simulations studies showed that in wtp53 OD, the residue Arg337 forms three salt bridges with D352 (~40 %) (intradimer), E349 (~10 %) (intradimer), and E343 (~10 %) (interdimer) to stabilize the tetrameric state indicating the importance of Arg at 337th position (Table S1). Hence, a more profound structural and functional understanding of the p53 OD is required to develop therapeutic drugs against these mutants.

Abbreviations: *FTIR- Fourier Transform Infrared Spectroscopy, CD-Circular Dichroism, CTR- C-terminal region, OD-oligomerization domain, RD-regulatory domain, wt-wild type.*

CRediT authorship contribution statement

Alankrita Singh: Methodology, Investigation, Validation, Visualization, Formal analysis, Writing-Original Draft, Writing-Review & Editing. **Lakshay Malhotra:** Methodology, Investigation, Validation, Visualization, Formal analysis, Writing-Original Draft, Writing-Review & Editing. **Abhay Mishra:** FTIR data collection. **Simran Kundral:** wtp53 CTR cloning. **Pawan Kumar Tiwari:** wtp53 CTR cloning. **Saroj Kumar:** Supervision. **Hariprasad Gururao:** Formal analysis and validation. **Punit Kaur:** Supervision. **Abdul Samath Ethayathulla:** Conceptualization, Methodology, Validation, Formal analysis, Writing - Original Draft, Writing - Review & Editing, Visualization, Resources, Funding Acquisition, and Supervision.

Declaration of competing interest

All authors declare they have no conflict of interest.

Acknowledgments

AS is thankful to the Department of Biotechnology (DBT) for providing the Junior Research Fellowship (DBT/2021-22/AIIMS/1639). **ASE** is thankful to the Indian Council of Medical Research (ICMR) for the financial assistance of the project (grant ID No: 5/13/72/2020/NCD-III) and the All India Institute of Medical Sciences (AIIMS) for providing the facility.

Appendix A. Supplementary data

Supplementary data to this article can be found online at https://doi.org/10.1016/j.abb.2025.110381.

Data availability

Data will be made available on request.

References

[1] B.J. Aubrey, A. Strasser, G.L. Kelly, Tumor-suppressor functions of the TP53 pathway, Cold Spring Harb. Perspect. Med. 6 (2016) a026062, https://doi.org/10.1101/cshperspect.a026062.
[2] C.A. Finlay, P.W. Hinds, A.J. Levine, The p53 proto-oncogene can act as a suppressor of transformation, Cell 57 (1989) 1083–1093, https://doi.org/10.1016/0092-8674(89)90045-7.
[3] B.J. Hwang, J.M. Ford, P.C. Hanawalt, G. Chu, Expression of the p48 xeroderma pigmentosum gene is p53-dependent and is involved in global genomic repair, Proc. Natl. Acad. Sci. U. S. A 96 (1999) 424–428, https://doi.org/10.1073/pnas.96.2.424.
[4] M.L. Smith, J.M. Ford, M.C. Hollander, R.A. Bortnick, S.A. Amundson, Y.R. Seo, C.X. Deng, P.C. Hanawalt, A.J. Fornace, p53-mediated DNA repair responses to UV radiation: studies of mouse cells lacking p53, p21, and/or gadd45 genes, Mol. Cell Biol. 20 (2000) 3705–3714, https://doi.org/10.1128/MCB.20.10.3705-3714.2000.
[5] S.A. Amundson, A. Patterson, K.T. Do, A.J. Fornace, A nucleotide excision repair master-switch: p53 regulated coordinate induction of global genomic repair genes, Cancer Biol. Ther. 1 (2002) 145–149, https://doi.org/10.4161/cbt.59.
[6] M.E. Fitch, I.V. Cross, S.J. Turner, S. Adimoolam, C.X. Lin, K.G. Williams, J. M. Ford, The DDB2 nucleotide excision repair gene product p48 enhances global genomic repair in p53 deficient human fibroblasts, DNA Repair 2 (2003) 819–826, https://doi.org/10.1016/s1568-7864(03)00066-1.
[7] L.R. Livingstone, A. White, J. Sprouse, E. Livanos, T. Jacks, T.D. Tlsty, Altered cell cycle arrest and gene amplification potential accompany loss of wild-type p53, Cell 70 (1992) 923–935, https://doi.org/10.1016/0092-8674(92)90243-6.
[8] Y. Yin, M.A. Tainsky, F.Z. Bischoff, L.C. Strong, G.M. Wahl, Wild-type p53 restores cell cycle control and inhibits gene amplification in cells with mutant p53 alleles, Cell 70 (1992) 937–948, https://doi.org/10.1016/0092-8674(92)90244-7.
[9] H. Hermeking, C. Lengauer, K. Polyak, T.C. He, L. Zhang, S. Thiagalingam, K. W. Kinzler, B. Vogelstein, 14-3-3sigma is a p53-regulated inhibitor of G2/M progression, Mol. Cell 1 (1997) 3–11, https://doi.org/10.1016/s1097-2765(00)80002-7.
[10] C.M. Eischen, M.F. Roussel, S.J. Korsmeyer, J.L. Cleveland, Bax loss impairs Myc-induced apoptosis and circumvents the selection of p53 mutations during Myc-

mediated lymphomagenesis, Mol. Cell Biol. 21 (2001) 7653–7662, https://doi.org/10.1128/MCB.21.22.7653-7662.2001.
[11] J.R. Jeffers, E. Parganas, Y. Lee, C. Yang, J. Wang, J. Brennan, K.H. MacLean, J. Han, T. Chittenden, J.N. Ihle, P.J. McKinnon, J.L. Cleveland, G.P. Zambetti, Puma is an essential mediator of p53-dependent and -independent apoptotic pathways, Cancer Cell 4 (2003) 321–328, https://doi.org/10.1016/s1535-6108(03)00244-7.
[12] A. Villunger, E.M. Michalak, L. Coultas, F. Müllauer, G. Böck, M.J. Ausserlechner, J.M. Adams, A. Strasser, p53- and drug-induced apoptotic responses mediated by BH3-only proteins puma and noxa, Science 302 (2003) 1036–1038, https://doi.org/10.1126/science.1090072.
[13] M.B. Kastan, O. Onyekwere, D. Sidransky, B. Vogelstein, R.W. Craig, Participation of p53 protein in the cellular response to DNA damage, Cancer Res. 51 (1991) 6304–6311.
[14] M.B. Kastan, Q. Zhan, W.S. el-Deiry, F. Carrier, T. Jacks, W.V. Walsh, B. S. Plunkett, B. Vogelstein, A.J. Fornace, A mammalian cell cycle checkpoint pathway utilizing p53 and GADD45 is defective in ataxia-telangiectasia, Cell 71 (1992) 587–597, https://doi.org/10.1016/0092-8674(92)90593-2.
[15] S.-J. Kim, S.-G. Hwang, D.Y. Shin, S.-S. Kang, J.-S. Chun, p38 kinase regulates nitric oxide-induced apoptosis of articular chondrocytes by accumulating p53 via NFkappa B-dependent transcription and stabilization by serine 15 phosphorylation, J. Biol. Chem. 277 (2002) 33501–33508, https://doi.org/10.1074/jbc.M202862200.
[16] A.C. Joerger, A.R. Fersht, Structural biology of the tumor suppressor p53, Annu. Rev. Biochem. 77 (2008) 557–582, https://doi.org/10.1146/annurev.biochem.77.060806.091238.
[17] C.-L. Wei, Q. Wu, V.B. Vega, K.P. Chiu, P. Ng, T. Zhang, A. Shahab, H.C. Yong, Y. Fu, Z. Weng, J. Liu, X.D. Zhao, J.-L. Chew, Y.L. Lee, V.A. Kuznetsov, W.-K. Sung, L.D. Miller, B. Lim, E.T. Liu, Q. Yu, H.-H. Ng, Y. Ruan, A global map of p53 transcription-factor binding sites in the human genome, Cell 124 (2006) 207–219, https://doi.org/10.1016/j.cell.2005.10.043.
[18] B. Ma, Y. Pan, J. Zheng, A.J. Levine, R. Nussinov, Sequence analysis of p53 response-elements suggests multiple binding modes of the p53 tetramer to DNA targets, Nucleic Acids Res. 35 (2007) 2986–3001, https://doi.org/10.1093/nar/gkm192.
[19] C.J. Thut, J.L. Chen, R. Klemm, R. Tjian, p53 transcriptional activation mediated by coactivators TAFII40 and TAFII60, Science 267 (1995) 100–104, https://doi.org/10.1126/science.7809597.
[20] K.K. Walker, A.J. Levine, Identification of a novel p53 functional domain that is necessary for efficient growth suppression, Proc. Natl. Acad. Sci. U. S. A 93 (1996) 15335–15340, https://doi.org/10.1073/pnas.93.26.15335.
[21] A.K. Nagaich, V.B. Zhurkin, S.R. Durell, R.L. Jernigan, E. Appella, R. E. Harrington, p53-induced DNA bending and twisting: p53 tetramer binds on the outer side of a DNA loop and increases DNA twisting, Proc. Natl. Acad. Sci. U. S. A 96 (1999) 1875–1880, https://doi.org/10.1073/pnas.96.5.1875.
[22] K. McKinney, M. Mattia, V. Gottifredi, C. Prives, p53 linear diffusion along DNA requires its C terminus, Mol. Cell 16 (2004) 413–424, https://doi.org/10.1016/j.molcel.2004.09.032.
[23] P. Balagurumoorthy, H. Sakamoto, M.S. Lewis, N. Zambrano, G.M. Clore, A. M. Gronenborn, E. Appella, R.E. Harrington, Four p53 DNA-binding domain peptides bind natural p53-response elements and bend the DNA, Proc. Natl. Acad. Sci. U. S. A 92 (1995) 8591–8595, https://doi.org/10.1073/pnas.92.19.8591.
[24] K.G. McLure, P.W. Lee, How p53 binds DNA as a tetramer, EMBO J. 17 (1998) 3342–3350, https://doi.org/10.1093/emboj/17.12.3342.
[25] T. Göhler, M. Reimann, D. Cherny, K. Walter, G. Warnecke, E. Kim, W. Deppert, Specific interaction of p53 with target binding sites is determined by DNA conformation and is regulated by the C-terminal domain, J. Biol. Chem. 277 (2002) 41192–41203, https://doi.org/10.1074/jbc.M202344200.
[26] A. Tafvizi, F. Huang, A.R. Fersht, L.A. Mirny, A.M. van Oijen, A single-molecule characterization of p53 search on DNA, Proc. Natl. Acad. Sci. U. S. A 108 (2011) 563–568, https://doi.org/10.1073/pnas.1016020107.
[27] L. Malhotra, A. Singh, P. Kaur, A.S. Ethayathulla, Comprehensive omics studies of p53 mutants in human cancer, Brief, Funct. Genomics 22 (2023) 97–108, https://doi.org/10.1093/bfgp/elac015.
[28] L. Malhotra, A. Singh, P. Kaur, A.S. Ethayathulla, Phenotypical mapping of TP53 unique missense mutations spectrum in human cancers, J. Biomol. Struct. Dyn. 0 (n.d.) 1–14. https://doi.org/10.1080/07391102.2024.2435060.
[29] L. Malhotra, A. Singh, P. Kaur, A.S. Ethayathulla, Phenotypical mapping of TP53 unique missense mutations spectrum in human cancers, 2023.02.06.527255, https://doi.org/10.1101/2023.02.06.527255, 2023.
[30] L. Bouaoun, D. Sonkin, M. Ardin, M. Hollstein, G. Byrnes, J. Zavadil, M. Olivier, TP53 variations in human cancers: new lessons from the IARC TP53 database and genomics data, Hum. Mutat. 37 (2016) 865–876, https://doi.org/10.1002/humu.23035.
[31] N.W. Fischer, A. Prodeus, J. Tran, D. Malkin, J. Gariépy, Association between the oligomeric status of p53 and clinical outcomes in Li-fraumeni syndrome, J. Natl. Cancer Inst. (Bethesda) 110 (2018) 1418–1421, https://doi.org/10.1093/jnci/djy114.
[32] D. Malkin, F.P. Li, L.C. Strong, J.F. Fraumeni, C.E. Nelson, D.H. Kim, J. Kassel, M. A. Gryka, F.Z. Bischoff, M.A. Tainsky, S.H. Friend, Germ line p53 mutations in a familial syndrome of breast cancer, sarcomas, and other neoplasms, Science 250 (1990) 1233–1238, https://doi.org/10.1126/science.1978757.
[33] A. Petitjean, M.I.W. Achatz, A.L. Borresen-Dale, P. Hainaut, M. Olivier, TP53 mutations in human cancers: functional selection and impact on cancer prognosis and outcomes, Oncogene 26 (2007) 2157–2165, https://doi.org/10.1038/sj.onc.1210302.
[34] R. Kamada, T. Nomura, C.W. Anderson, K. Sakaguchi, Cancer-associated p53 tetramerization domain mutants, J. Biol. Chem. 286 (2011) 252–258, https://doi.org/10.1074/jbc.M110.174698.
[35] N.W. Fischer, A. Prodeus, D. Malkin, J. Gariépy, p53 oligomerization status modulates cell fate decisions between growth, arrest and apoptosis, Cell Cycle 15 (2016) 3210–3219, https://doi.org/10.1080/15384101.2016.1241917.
[36] J. Gencel-Augusto, G. Lozano, p53 tetramerization: at the center of the dominant-negative effect of mutant p53, Genes Dev. 34 (2020) 1128–1146, https://doi.org/10.1101/gad.340976.120.
[37] E.C. Pietsch, J.I.-J. Leu, A. Frank, P. Dumont, D.L. George, M.E. Murphy, The tetramerization domain of p53 is required for efficient BAK oligomerization, Cancer Biol. Ther. 6 (2007) 1576–1583, https://doi.org/10.4161/cbt.6.10.4719.
[38] G.M. Clore, J. Ernst, R. Clubb, J.G. Omichinski, W.M. Kennedy, K. Sakaguchi, E. Appella, A.M. Gronenborn, Refined solution structure of the oligomerization domain of the tumour suppressor p53, Nat. Struct. Biol. 2 (1995) 321–333, https://doi.org/10.1038/nsb0495-321.
[39] P.D. Jeffrey, S. Gorina, N.P. Pavletich, Crystal structure of the tetramerization domain of the p53 tumor suppressor at 1.7 angstroms, Science 267 (1995) 1498–1502, https://doi.org/10.1126/science.7878469.
[40] S. Kato, S.-Y. Han, W. Liu, K. Otsuka, H. Shibata, R. Kanamaru, C. Ishioka, Understanding the function–structure and function–mutation relationships of p53 tumor suppressor protein by high-resolution missense mutation analysis, Proc. Natl. Acad. Sci. USA 100 (2003) 8424–8429, https://doi.org/10.1073/pnas.1431692100.
[41] T. Kawaguchi, S. Kato, K. Otsuka, G. Watanabe, T. Kumabe, T. Tominaga, T. Yoshimoto, C. Ishioka, The relationship among p53 oligomer formation, structure and transcriptional activity using a comprehensive missense mutation library, Oncogene 24 (2005) 6976–6981, https://doi.org/10.1038/sj.onc.1208839.
[42] The TP53 Database | ISB-CGC, (n.d.). https://tp53.isb-cgc.org/(accessed July 22, 2024).
[43] C. Rollenhagen, P. Chène, Characterization of p53 mutants identified in human tumors with a missense mutation in the tetramerization domain, Int. J. Cancer 78 (1998) 372–376, https://doi.org/10.1002/(SICI)1097-0215(19981029)78:3<372::AID-IJC19>3.0.CO;2-8.
[44] R. Kulikov, M. Winter, C. Blattner, Binding of p53 to the central domain of Mdm2 is regulated by phosphorylation, J. Biol. Chem. 281 (2006) 28575–28583, https://doi.org/10.1074/jbc.M513311200.
[45] T. Imagawa, T. Terai, Y. Yamada, R. Kamada, K. Sakaguchi, Evaluation of transcriptional activity of p53 in individual living mammalian cells, Anal. Biochem. 387 (2009) 249–256, https://doi.org/10.1016/j.ab.2009.01.030.
[46] Y. Itahana, H. Ke, Y. Zhang, p53 Oligomerization is essential for its C-terminal lysine acetylation, J. Biol. Chem. 284 (2009) 5158–5164, https://doi.org/10.1074/jbc.M805696200.
[47] G.K. Annor, N. Elshabassy, D. Lundine, D.-G. Conde, G. Xiao, V. Ellison, J. Bargonetti, Oligomerization of mutant p53 R273H is not required for gain-of-function chromatin associated activities, Front. Cell Dev. Biol. 9 (2021) 772315, https://doi.org/10.3389/fcell.2021.772315.
[48] T.S. Davison, P. Yin, E. Nie, C. Kay, C.H. Arrowsmith, Characterization of the oligomerization defects of two p53 mutants found in families with Li-Fraumeni and Li-Fraumeni-like syndrome, Oncogene 17 (1998) 651–656, https://doi.org/10.1038/sj.onc.1202062.
[49] M.E. Lomax, D.M. Barnes, T.R. Hupp, S.M. Picksley, R.S. Camplejohn, Characterization of p53 oligomerization domain mutations isolated from Li-Fraumeni and Li-Fraumeni like family members, Oncogene 17 (1998) 643–649, https://doi.org/10.1038/sj.onc.1201974.
[50] M.E. Lomax, D.M. Barnes, R. Gilchrist, S.M. Picksley, J.M. Varley, R. S. Camplejohn, Two functional assays employed to detect an unusual mutation in the oligomerisation domain of p53 in a Li-Fraumeni like family, Oncogene 14 (1997) 1869–1874, https://doi.org/10.1038/sj.onc.1201133.
[51] J. Malcikova, B. Tichy, J. Damborsky, J. Kabathova, M. Trbusek, J. Mayer, S. Pospisilova, Analysis of the DNA-binding activity of p53 mutants using functional protein microarrays and its relationship to transcriptional activation, Biol. Chem. 391 (2010) 197–205, https://doi.org/10.1515/bc.2010.027.
[52] J. Atz, P. Wagner, K. Roemer, Function, oligomerization, and conformation of tumor-associated p53 proteins with mutated C-terminus, J. Cell. Biochem. 76 (2000) 572–584, https://doi.org/10.1002/(sici)1097-4644(20000315)76:4<572::aid-jcb6>3.0.co;2-6.
[53] J.J. Jordan, A. Inga, K. Conway, S. Edmiston, L.A. Carey, L. Wu, M.A. Resnick, Altered-function p53 missense mutations identified in breast cancers can have subtle effects on transactivation, Mol. Cancer Res. MCR 8 (2010) 701–716, https://doi.org/10.1158/1541-7786.MCR-09-0442.
[54] J. Slovackova, D. Grochova, J. Navratilova, J. Smarda, J. Smardova, Transactivation by temperature-dependent p53 mutants in yeast and human cells, Cell Cycle Georget, Text 9 (2010) 2141–2148, https://doi.org/10.4161/cc.9.11.11808.
[55] M. Rigoli, G. Spagnolli, G. Lorengo, P. Monti, R. Potestio, E. Biasini, A. Inga, Structural basis of mutation-dependent p53 tetramerization deficiency, Int. J. Mol. Sci. 23 (2022) 7960, https://doi.org/10.3390/ijms23147960.
[56] R. Bansal, M.A. Haque, M.I. Hassan, A.S. Ethayathulla, P. Kaur, Structural and conformational behavior of MurE ligase from Salmonella enterica serovar Typhi at different temperature and pH conditions, Int. J. Biol. Macromol. 150 (2020) 389–399, https://doi.org/10.1016/j.ijbiomac.2020.01.306.
[57] C.A. Luer, K.-P. Wong, The effects of pH and temperature on the circular dichroism of human erythrocyte membranes, Biophys. Chem. 9 (1978) 15–22, https://doi.org/10.1016/0301-4622(78)87011-2.

[58] L. Malhotra, S. Sharma, G. Hariprasad, R. Dhingra, V. Mishra, R.S. Sharma, P. Kaur, A.S. Ethayathulla, Mechanism of apoptosis activation by Curcumin rescued mutant p53Y220C in human pancreatic cancer, Biochim. Biophys. Acta Mol. Cell Res. 1869 (2022) 119343, https://doi.org/10.1016/j.bbamcr.2022.119343.

[59] L. Malhotra, H.K.V. Goyal, S. Jhuria, K. Dev, S. Kumar, M. Kumar, P. Kaur, A. S. Ethayathulla, Curcumin rescue p53Y220C in BxPC-3 pancreatic adenocarcinomas cell line: evidence-based on computational, biophysical, and in vivo studies, Biochim. Biophys. Acta Gen. Subj. 1865 (2021) 129807, https://doi.org/10.1016/j.bbagen.2020.129807.

[60] A. Micsonai, É. Moussong, F. Wien, E. Boros, H. Vadászi, N. Murvai, Y.-H. Lee, T. Molnár, M. Réfrégiers, Y. Goto, Á. Tantos, J. Kardos, BeStSel: webserver for secondary structure and fold prediction for protein CD spectroscopy, Nucleic Acids Res. 50 (2022) W90–W98, https://doi.org/10.1093/nar/gkac345.

[61] A. Micsonai, É. Bulyáki, J. Kardos, BeStSel: from secondary structure analysis to protein fold prediction by circular dichroism spectroscopy, in: Y.W. Chen, C.-P. B. Yiu (Eds.), Struct. Genomics Gen. Appl., Springer US, New York, NY, 2021, pp. 175–189, https://doi.org/10.1007/978-1-0716-0892-0_11.

[62] A. Micsonai, F. Wien, É. Bulyáki, J. Kun, É. Moussong, Y.-H. Lee, Y. Goto, M. Réfrégiers, J. Kardos, BeStSel: a web server for accurate protein secondary structure prediction and fold recognition from the circular dichroism spectra, Nucleic Acids Res. 46 (2018) W315–W322, https://doi.org/10.1093/nar/gky497.

[63] A. Micsonai, F. Wien, É. Bulyáki, J. Kun, É. Moussong, Y.-H. Lee, Y. Goto, M. Réfrégiers, J. Kardos, BeStSel: a web server for accurate protein secondary structure prediction and fold recognition from the circular dichroism spectra, Nucleic Acids Res. 46 (2018) W315–W322, https://doi.org/10.1093/nar/gky497.

[64] C.M. Johnson, Differential scanning calorimetry as a tool for protein folding and stability, Arch. Biochem. Biophys. 531 (2013) 100–109, https://doi.org/10.1016/j.abb.2012.09.008.

[65] J.M. Sanchez-Ruiz, Differential scanning calorimetry of proteins, in: B.B. Biswas, S. Roy (Eds.), Proteins Struct. Funct. Eng., Springer, US, Boston, MA, 1995, pp. 133–176, https://doi.org/10.1007/978-1-4899-1727-0_6.

[66] L. Malhotra, P. Kaur, A.S. Ethayathulla, Flavonoids as potential reactivators of structural mutation p53Y220C by computational and cell-based studies, J. Biomol. Struct. Dyn. 42 (2024) 9602–9613. https://doi.org/10.1080/07391102.2023.2252071.

[67] A.M. Londhe, C.G. Gadhe, S.M. Lim, A.N. Pae, Investigation of molecular details of keap1-nrf2 inhibitors using molecular dynamics and umbrella sampling techniques, Molecules 24 (2019) 4085, https://doi.org/10.3390/molecules24224085.

[68] M. Motiwale, N.S. Yadav, S. Kumar, T. Kushwaha, G. Choudhir, S. Sharma, P. K. Singour, Finding potent inhibitors for COVID-19 main protease (Mpro): an in silico approach using SARS-CoV-3CL protease inhibitors for combating CORONA, J. Biomol. Struct. Dyn. 40 (2022) 1534–1545, https://doi.org/10.1080/07391102.2020.1829501.

[69] D.J. Wales, T.V. Bogdan, Potential energy and free energy landscapes, J. Phys. Chem. B 110 (2006) 20765–20776, https://doi.org/10.1021/jp0680544.

[70] A. Di Ianni, C. Tüting, M. Kipping, C.H. Ihling, J. Köppen, C. Iacobucci, C. Arlt, P. L. Kastritis, A. Sinz, Structural assessment of the full-length wild-type tumor suppressor protein p53 by mass spectrometry-guided computational modeling, Sci. Rep. 13 (2023) 8497, https://doi.org/10.1038/s41598-023-35437-5.

[71] C. Arlt, V. Flegler, C.H. Ihling, M. Schäfer, I. Thondorf, A. Sinz, An integrated mass spectrometry based approach to probe the structure of the full-length wild-type tetrameric p53 tumor suppressor, Angew. Chem. Int. Ed. 56 (2017) 275–279, https://doi.org/10.1002/anie.201609826.

[72] M. D'Abramo, N. Bešker, A. Desideri, A.J. Levine, G. Melino, G. Chillemi, The p53 tetramer shows an induced-fit interaction of the C-terminal domain with the DNA-binding domain, Oncogene 35 (2016) 3272–3281, https://doi.org/10.1038/onc.2015.388.

[73] D.B. Veprintsev, A.R. Fersht, Algorithm for prediction of tumour suppressor p53 affinity for binding sites in DNA, Nucleic Acids Res. 36 (2008) 1589–1598, https://doi.org/10.1093/nar/gkm1040.

[74] N. Pham, A. Lucumi, N. Cheung, H. Viadiu, The tetramer of p53 in the absence of DNA forms a relaxed quaternary state, Biochemistry 51 (2012) 8053–8055, https://doi.org/10.1021/bi301193k.

[75] A.S. Krois, S. Park, M.A. Martinez-Yamout, H.J. Dyson, P.E. Wright, Mapping interactions of the intrinsically disordered C-terminal regions of tetrameric p53 by segmental isotope labeling and NMR, Biochemistry 61 (2022) 2709–2719, https://doi.org/10.1021/acs.biochem.2c00528.

[76] O. Laptenko, I. Shiff, W. Freed-Pastor, A. Zupnick, M. Mattia, E. Freulich, I. Shamir, N. Kadouri, T. Kahan, J. Manfredi, I. Simon, C. Prives, The p53 C terminus controls site-specific DNA binding and promotes structural changes within the central DNA binding domain, Mol. Cell 57 (2015) 1034–1046, https://doi.org/10.1016/j.molcel.2015.02.015.

[77] A.C. Joerger, S. Rajagopalan, E. Natan, D.B. Veprintsev, C.V. Robinson, A. R. Fersht, Structural evolution of p53, p63, and p73: implication for heterotetramer formation, Proc. Natl. Acad. Sci. U. S. A (2009), https://doi.org/10.1073/pnas.0905867106.

[78] G.M. Clore, J. Ernst, R. Clubb, J.G. Omichinski, W.M. Kennedy, K. Sakaguchi, E. Appella, A.M. Gronenborn, Refined solution structure of the oligomerization domain of the tumour suppressor p53, Nat. Struct. Biol. 2 (1995) 321–333, https://doi.org/10.1038/nsb0495-321.

[79] G.M. Clore, J.G. Omichinski, K. Sakaguchi, N. Zambrano, H. Sakamoto, E. Appella, A.M. Gronenborn, High-resolution structure of the oligomerization domain of p53 by multidimensional NMR, Science 265 (1994) 386–391, https://doi.org/10.1126/science.8023159.

[80] P.R. Mittl, P. Chène, M.G. Grütter, Crystallization and structure solution of p53 (residues 326-356) by molecular replacement using an NMR model as template, Acta Crystallogr. D Biol. Crystallogr. 54 (1998) 86–89, https://doi.org/10.1107/s0907444997006550.

[81] S. Sakaguchi, N. Nakagawa, H.M. Wahba, J. Wada, R. Kamada, J.G. Omichinski, K. Sakaguchi, Highly similar tetramerization domains from the p53 protein of different mammalian species possess varying biophysical, functional and structural properties, Int. J. Mol. Sci. 24 (2023) 16620, https://doi.org/10.3390/ijms242316620.

[82] P. Chène, The role of tetramerization in p53 function, Oncogene 20 (2001) 2611–2617, https://doi.org/10.1038/sj.onc.1204373.

[83] G. Gaglia, Y. Guan, J.V. Shah, G. Lahav, Activation and control of p53 tetramerization in individual living cells, Proc. Natl. Acad. Sci. U. S. A 110 (2013) 15497–15501, https://doi.org/10.1073/pnas.1311126110.

[84] K. Sakaguchi, H. Sakamoto, M.S. Lewis, C.W. Anderson, J.W. Erickson, E. Appella, D. Xie, Phosphorylation of serine 392 stabilizes the tetramer formation of tumor suppressor protein p53, Biochemistry 36 (1997) 10117–10124, https://doi.org/10.1021/bi970759w.

[85] J.M. Stommel, N.D. Marchenko, G.S. Jimenez, U.M. Moll, T.J. Hope, G.M. Wahl, A leucine-rich nuclear export signal in the p53 tetramerization domain: regulation of subcellular localization and p53 activity by NES masking, EMBO J. 18 (1999) 1660–1672, https://doi.org/10.1093/emboj/18.6.1660.

[86] Z. Che, H. Sun, W. Yao, B. Lu, Q. Han, Role of post-translational modifications in regulation of tumor suppressor p53 function, Front. Oral Maxillofac. Med. 2 (2020), https://doi.org/10.21037/fomm.2019.12.02.

[87] B. Gu, W.-G. Zhu, Surf the post-translational modification network of p53 regulation, Int. J. Biol. Sci. 8 (2012) 672–684, https://doi.org/10.7150/ijbs.4283.

[88] Y. Liu, O. Tavana, W. Gu, p53 modifications: exquisite decorations of the powerful guardian, J. Mol. Cell Biol. 11 (2019) 564–577, https://doi.org/10.1093/jmcb/mjz060.

[89] J. Wen, D. Wang, Deciphering the PTM codes of the tumor suppressor p53, J. Mol. Cell Biol. 13 (2022) 774–785, https://doi.org/10.1093/jmcb/mjab047.

[90] M. Jansson, S.T. Durant, E.-C. Cho, S. Sheahan, M. Edelmann, B. Kessler, N.B. La Thangue, Arginine methylation regulates the p53 response, Nat. Cell Biol. 10 (2008) 1431–1439, https://doi.org/10.1038/ncb1802.

[91] C.D. Knights, J. Catania, S.D. Giovanni, S. Muratoglu, R. Perez, A. Swartzbeck, A. A. Quong, X. Zhang, T. Beerman, R.G. Pestell, M.L. Avantaggiati, Distinct p53 acetylation cassettes differentially influence gene-expression patterns and cell fate, J. Cell Biol. 173 (2006) 533–544, https://doi.org/10.1083/jcb.200512059.

[92] N.W. Fischer, A. Prodeus, D. Malkin, J. Gariépy, p53 oligomerization status modulates cell fate decisions between growth, arrest and apoptosis, Cell Cycle 15 (2016) 3210–3219, https://doi.org/10.1080/15384101.2016.1241917.

[93] R. Kamada, T. Nomura, C.W. Anderson, K. Sakaguchi, Cancer-associated p53 tetramerization domain mutants: quantitative analysis reveals a low threshold for tumor suppressor inactivation, J. Biol. Chem. 286 (2011) 252–258, https://doi.org/10.1074/jbc.M110.174698.

[94] M. Retzlaff, J. Rohrberg, N.J. Küpper, S. Lagleder, A. Bepperling, F. Manzenrieder, J. Peschek, H. Kessler, J. Buchner, The regulatory domain stabilizes the p53 tetramer by intersubunit contacts with the DNA binding domain, J. Mol. Biol. 425 (2013) 144–155, https://doi.org/10.1016/j.jmb.2012.10.015.

[95] S. Bell, C. Klein, L. Müller, S. Hansen, J. Buchner, p53 contains large unstructured regions in its native state, J. Mol. Biol. 322 (2002) 917–927, https://doi.org/10.1016/s0022-2836(02)00848-3.

[96] A. Kumar, P. Kumar, S. Kumari, V.N. Uversky, R. Giri, Folding and structural polymorphism of p53 C-terminal domain: one peptide with many conformations, Arch. Biochem. Biophys. 684 (2020) 108342, https://doi.org/10.1016/j.abb.2020.108342.

[97] M. Ashcroft, Y. Taya, K.H. Vousden, Stress signals utilize multiple pathways to stabilize p53, Mol. Cell Biol. 20 (2000) 3224–3233, https://doi.org/10.1128/MCB.20.9.3224-3233.2000.

[98] J. Smith, L.M. Tho, N. Xu, D.A. Gillespie, The ATM-Chk2 and ATR-Chk1 pathways in DNA damage signaling and cancer, Adv. Cancer Res. 108 (2010) 73–112, https://doi.org/10.1016/B978-0-12-380888-2.00003-0.

[99] W.R. Taylor, G.R. Stark, Regulation of the G2/M transition by p53, Oncogene 20 (2001) 1803–1815, https://doi.org/10.1038/sj.onc.1204252.

[100] S. Chuikov, J.K. Kurash, J.R. Wilson, B. Xiao, N. Justin, G.S. Ivanov, K. McKinney, P. Tempst, C. Prives, S.J. Gamblin, N.A. Barlev, D. Reinberg, Regulation of p53 activity through lysine methylation, Nature 432 (2004) 353–360, https://doi.org/10.1038/nature03117.

[101] A. Ito, C.-H. Lai, X. Zhao, S. Saito, M.H. Hamilton, E. Appella, T.-P. Yao, p300/CBP-mediated p53 acetylation is commonly induced by p53-activating agents and inhibited by MDM2, EMBO J. 20 (2001) 1331–1340, https://doi.org/10.1093/emboj/20.6.1331.

[102] N.W. Fischer, A. Prodeus, J. Tran, D. Malkin, J. Gariépy, Association between the oligomeric status of p53 and clinical outcomes in Li-fraumeni syndrome, JNCI J. Natl. Cancer Inst. 110 (2018) 1418–1421, https://doi.org/10.1093/jnci/djy114.